J. Electrochem. Sci. Eng. **13(1)** (2023) 149-162; https://dx.doi.org/10.5599/jese.1391

Open Access : : ISSN 1847-9286
https://pub.iapchem.org/ojs/index.php/JESE

Original scientific paper

Tool wear rate during electrical discharge machining for aluminium metal matrix composite prepared by squeeze casting: A prospect as a biomaterial

Arvinder Singh Channi[1], Harminder Singh Bains[2], Jasmaninder Singh Grewal[3], Vettivel Singaravel Chidambaranthan[4] and Raman Kumar[5,✉]

[1]*Department of Mechanical Engineering, IKG Punjab Technical University, Jalandhar, Punjab, India*
[2]*Department of Mechanical Engineering, University Institute of Engineering and Technology, Panjab University SSG Regional Centre Hoshiarpur, Punjab, India*
[3]*Department of Mechanical and Production Engineering, Guru Nanak Dev Engineering College, Ludhiana, Punjab, India*
[4]*Department-Mechanical Engineering, CCET (Degree Wing), Chandigarh, India*
[5]*Department of Mechanical and Production Engineering, Guru Nanak Dev Engineering College, Ludhiana, Punjab 141006, India*

Corresponding author: ✉sehgal91@yahoo.co.in

Received: May 29, 2022; Accepted: June 11, 2022; Published: August 29, 2022

Abstract

Squeeze casting was used to prepare aluminium alloy-6061/titanium diboride (TiB_2) to create a composite with varied TiB_2 quantities. The metallographic structure, tensile strength, and hardness of the composite have been explored. The tensile strength and hardness of produced metal matrix composites increased when a particle of TiB_2 was increased from 5 to 10 vol.%. This study uses electrical discharge machining (EDM) to investigate the output response tool wear rate (TWR). Variables in EDM operation were investigated, such as current, pulse on time, and voltage gap. The experiments were designed using the Box–Behnken strategy. Statistical approaches were used to analyse the experiments. At ideal settings for TiB_2 concentrations of 5 and 10 vol.%, TWR was 0.2146 and 0.1749 mm^3 min^{-1} and surface roughness was 2.47 and 3.03 µm, respectively. TiB_2 is utilized in automobile disc brakes, an industry where components slide against each other. The aluminium alloy-6061/titanium diboride has many applications as biomaterial and good prospect.

Keywords

Box Behnken design; hardness; tensile strength; response surface methodology; desirability analysis

Introduction

Metal matrix composites (MMCs) are increasingly used in structure, wear, thermal, transport, and electrical applications. Composites have better strength-to-weight and strength-to-cost ratios than similar monolithic conventional alloys [1]. Aluminium-based particulate matrix composite

composites have been recognized as an important class of materials used in the aircraft, vehicle, chemical, and automotive sectors due to their enhanced strength, high elastic modulus, and continued increased abrasion resistance over traditional base alloys [2]. There are three production procedures for aluminium MMCs liquid state, semisolid, and powder metallurgy [3]. First, the ceramic particles are integrated into a molten metallic matrix in liquid state techniques, and the MMC is cast. Stir Casting is a liquid state composite material fabrication process that involves mechanically stirring a ceramic particle into a molten matrix metal. The liquid composite material is subsequently cast using typical casting processes [4]. Aluminium 6061 is a low-density, more significant, and wear-resistant metal alloy. To counteract this fault, TiB_2 additives are formed to the alloy, enhancing its hardness, young's modulus, and abrasive wear resistance [5].

Aluminium alloys are reinforced with ceramic materials such as SiC, TiC, TiB_2, ZrB_2, AlN, Si_3N_4, Al_2O_3, and SiO_2. TiB_2, a reinforcing ceramic particle with a high Young's modulus, low density, and better Vickers hardness, is particularly appealing, thermal conductivity, high electrical conductivity, High elastic modulus, hardness, high melting point, superior wear resistance, and good thermal stability [6]. Studies show that TiB_2 particles do not react with aluminium [7]. As a result, brittle reactions at the reinforcement–matrix contact are avoided [8]. The behaviour of aluminium reinforced with TiC, TiB_2, B_4C, and SiC was compared utilizing the powder metallurgy approach [9]. TiB_2 outperformed the other reinforcements in terms of mechanical properties. TiB_2 is frequently used in advanced engineering ceramics due to its unique qualities [10].

The bioceramics are either strongly connected to the body's possessed materials or are nigh-indestructible metal oxides [11]. Dental and bone implants made of ceramics are increasingly widely used in healthcare. Surgical cermets are frequently utilized. Bioceramic coatings are routinely used on joint replacements to minimize wear and inflammation [12]. Bioceramics are also used in pacemakers, kidney dialysis machines, and respirators, among other medical applications [13]. Bioceramics are intended for endovascular circulation systems such as dialysis or designed bioreactors; otherwise, they are most commonly employed as implants. Because of their Physico-chemical properties, ceramics have many uses as biomaterials [14]. Alumina (Al_2O_3) is often used in bioceramics because it lasts longer than the patients. Middle ear ossicles, ocular prostheses, electrical insulating for implantable devices, catheter holes, and countless prototypes of implanted technologies such as cardiac pumps can all benefit from the material [15].

Nevertheless, porous materials have lesser mechanical strength than bone, making porous implants fragile. In addition, the implant can induce mechanical stresses at the tissue interface because the elastic modulus of ceramic materials is often higher than that of the surrounding bone tissue [16]. Biologically active ceramics have already seen particular usage responsible for biological reactivity, in contrast to their typical qualities. Instances include calcium phosphates, oxides, and hydroxides [17]. Bioceramics are suitable for medical use because they are anticorrosive, biocompatible, and attractive. Bioinertness and noncytotoxicity are two properties of zirconia ceramic. Carbon is another mechanical option that includes the after-bone and blood compatibility, no tissue reactivity, and no cell toxicity [18,19].

Due to the apparent geometric structure sophistication, high cutting costs, and high tool wear, manufacturing materials with reinforcement using traditional machining processes is difficult. As an outcome, non-traditional cutting processes for shaping metal matrix composites for a complex die contour have been developed [20]. Electric discharge machining (EDM)has become one of the most prevalent non-conventional methodologies. Electrically conductive materials are machined with EDM employing finely regulated sparks between an electrode and the workpiece in a dielectric fluid

media [21]. Using an artificial bee colony technique, researchers looked at numerous process parameter combinations to find the best material removal rate MRR and surface roughness (R_a) for EDM of EN31 tool steel. They also looked into the effects of machining parameters on machining performances, finding that when T–ON and current increased, so did MRR and R_a [22]. The EDM technique investigated the effects of voltage, current, T–ON, and duty factor on MRR, tool wear rate (TWR), and R_a. They devised a mathematical model for determining the average R_a, difficulty, and MRR. The calculated values are incredibly close to the experimental findings. As a result, the mathematical model can be utilized to analyse MRR and average R_a responses for parameter investigation [23]. In wire EDM of SS304, the output response of Ra and kerf-width were investigated for optimization [24]. According to ANOVA results, T–ON and peak currents substantially impact the surface quality of 2312 hot wrought steel [25]. In EDM process settings, the machining performance of AA7075 reinforced with SiC MMC with a copper tool electrode was investigated. T–ON is essential, contributing 57.9 % to performance measurements [26]. The central composite design optimized process parameters while considering MRR, TWR, and Ra during EDM. MRR increases as current increases, and TWR increases as peak current increases [27]. A genetic algorithm was utilized to explore the cutting properties of EDM during the machining of Al6351-B_4C-SiC MMC. The results reveal that current contributed 68.92 % in predicting R_a [28].

The impact of EDM process parameters on an MMC of AA 6061/SiC with a tool made of copper concluded that if the current was higher and voltage was lower, MRR reached its maximum. Conversely, when both current and voltage are low, R_a was improved [29]. The AA-6061/10% Al_2O_3 metal matrix composite machining properties were investigated using EDM. They managed the process parameters to achieve the highest MRR and lowest TWR possible. Analysis of variance is used to determine the optimal value of input parameters [30]. The effect of MMC of Al+TiB_2 fabricated by in-situ process and machined by EDM indicates that MRR increases with the current, while it decreases with the increases in reinforcement [31]. In machining Al/Cu/TiB_2 in-situ MMCs, a multi-criteria optimization technique was used to optimize the EDM parameter. MRR, TWR, and R_a are reaction parameters, while discharge current, pulse on time, and pulse off time are machining parameters. The study reveals that the optimized results agree with the confirmation run [32]. The effect of the EDM on the machining of the Al+TiB_2 using the copper electrode for MRR, TWR, and R_a indicates that MRR and TWR increase by increasing the current and spark ON time. It reduces with the increase of spark-off time, while R_a depends on the applied current and increases with the increase in the applied current [33]. Many studies were conducted on composite materials with EDM and achieved significant results [18,19,34-36].

A literature survey revealed that machining research for Al/TiB_2 composites had been conducted in some of the studies. On the other hand, The EDM of Al/TiB_2 squeeze cast composite on TWR has received little attention. This research aims to govern the effects of EDM process parameters such as current, pulse-on time, and voltage gap on TWR. The Box-Behnken method is used for the design of experiments. Response surface methodology (RSM) models were developed, supported with ANOVA, and verified with residual plots. The hardness and tensile strength (TS) were reported for a fabricated composite of AA 6061 with 5 and 10 vol.% TiB_2.

Experimental

Composite preparation

Aluminium 6061 alloy is one of the most extensively used materials in the Al6xxx series due to its high strength, outstanding workability, and excellent corrosion resistance [37]. On the other hand,

TiB_2 is a well-known ceramic material with exceptional properties [38-40]. As a result, the study's matrix is Al alloy 6061 reinforced with TiB_2. Hindalco's AA 6061 ingots were used as the matrix material, sliced into small pieces, and melted using TiB_2 of less than 10 microns. The SEM of Al 6061 is shown in Figure 1(a), and EDS is shown in Figure 1(b). Figure 1(c) shows the SEM of TiB_2, and Figure 1(d) depicts the EDS of TiB_2.

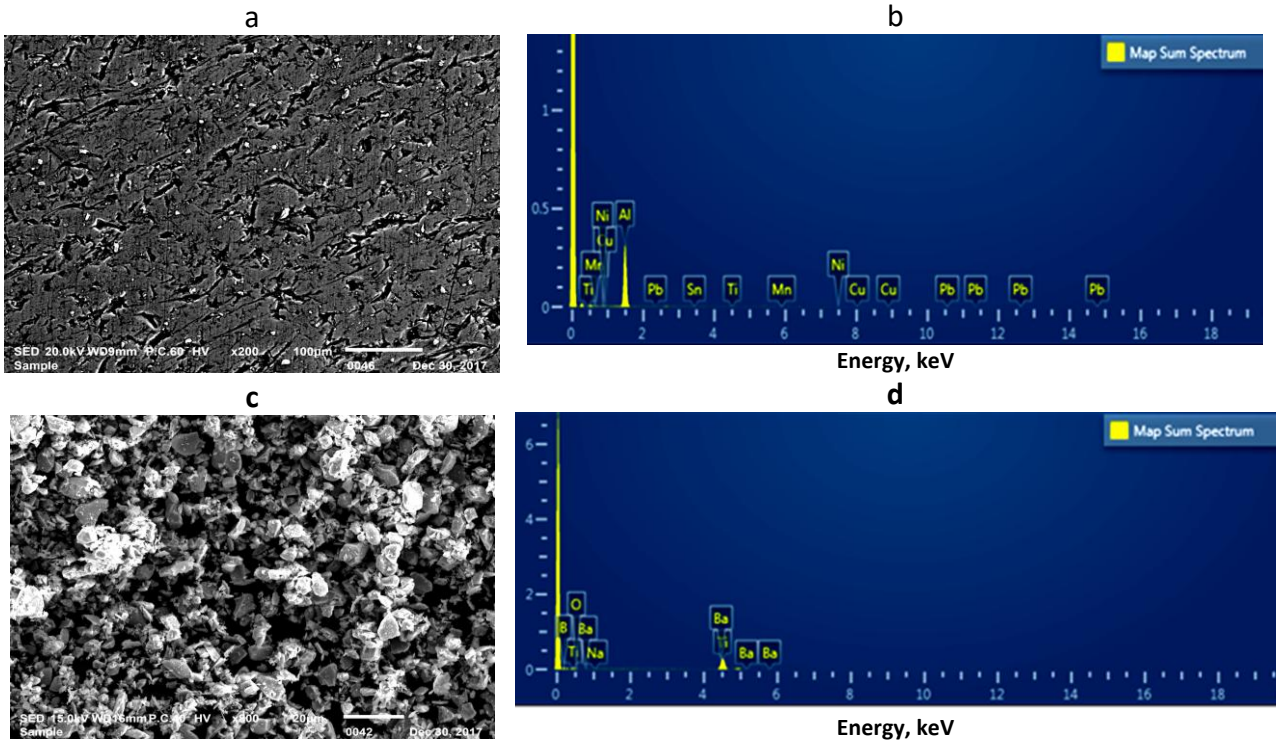

Figure 1. *(a) SEM of Al 6061, (b) EDS of AA 6061, (c) SEM of TiB_2, (d) EDS of TiB_2*

EDS analysis

Energy dispersive X-ray synthesis, or EDS analysis, is also known as energy dispersive X-ray microanalysis. It's an analytics method for identifying a sample's chemical composition or characterization. It is based on an interaction between an X-ray emitter and a specimen [41-43]. When applied to the ready samples with completely varied percentages of TiB_2, the EDS assessment provides the following results, as shown in Figure 2, and constituents of the EDS of AA6061 + TiB_2. Figure 2(a) AA6061+ 5 vol.% TiB_2 indicates the presence of aluminium, titanium, boron, and magnesium. Figure 2(b) AA6061 + 10 vol.% TiB_2 leads the aluminum, titanium, boron, chromium, and copper. Figures 2(c) and 2(d) show EDS layered images showing Ti and boron with uniform distribution.

Mechanical testing

Mechanical testing is a technique for determining a material's mechanical characteristics. It is used to assess a material regardless of its geometry and under specific topological situations [44-46].

Hardness and tensile strength test

The influence of TiB_2 particles on matrix hardness was investigated using a Vickers hardness tester on polished samples of produced AA 6061/TiB_2 specimens. The test was carried out following the ASTM E384-10 standard. In addition, hardness tests were performed at three different sites to safeguard the hard reinforcement particles from the indenter resting effect. The hardness of AA 6061 + 5 vol.% TiB_2 and AA6061 + 10 vol.% TiB_2 are shown in Table 1. The hardness of TiB_2 increases

as the percent volume of TiB_2 increases. The outcome of TS is depicted in Table 2. It is clear that with the increase in the content of the reinforcement, there is an increase in TS.

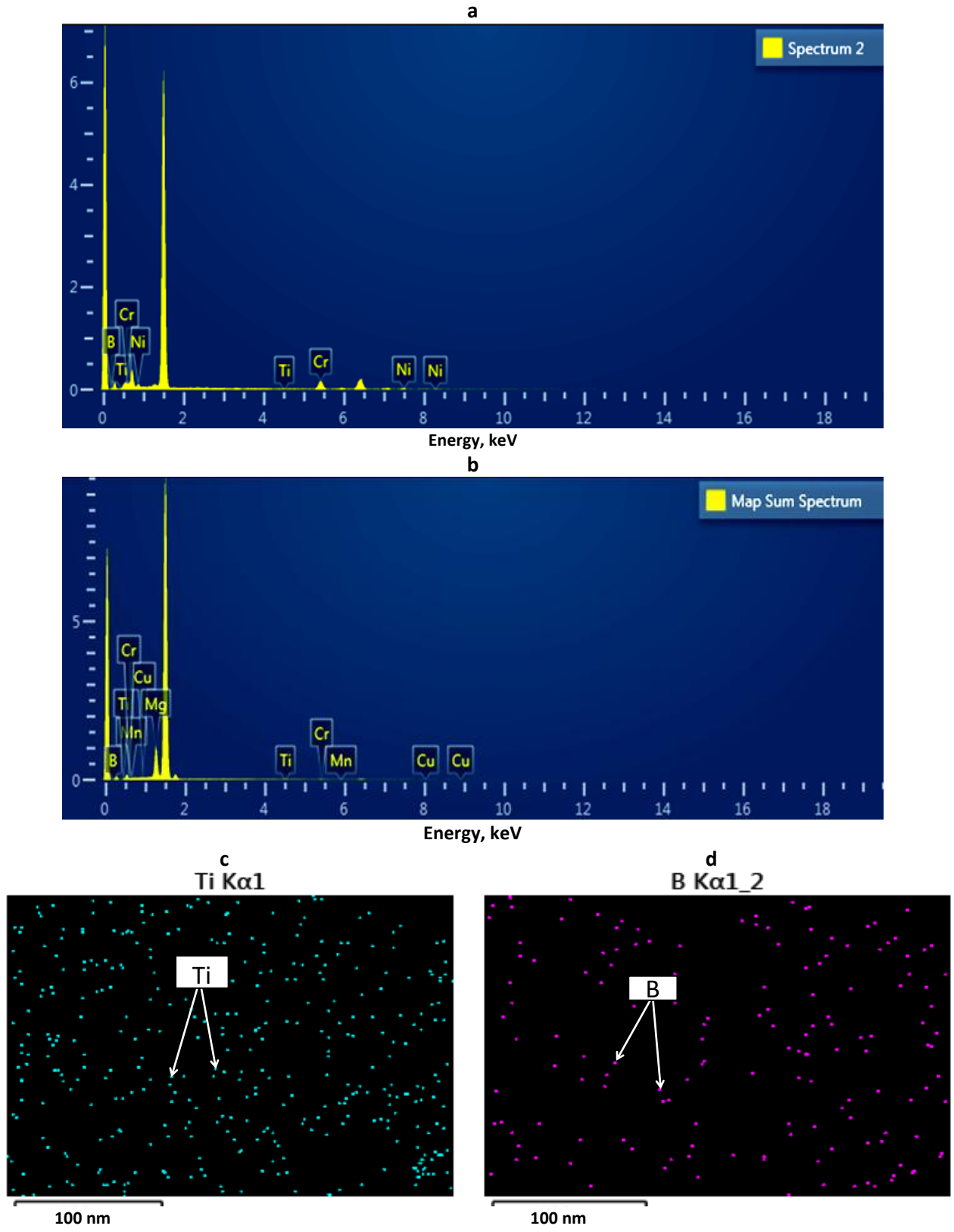

Figure 2. *EDS of composite specimens (a) AA6061 + 5 vol.% TiB_2; (b) AA6061 + 10 vol.% TiB_2; layered EDS image for (c) Ti and (d) boron*

Table 1. *Microhardness reading of MMC*

Sample	Microhardness, HV			
	Trial 1	Trial 2	Trial 3	Mean
AA6061+ 5 vol.% TiB_2	100.8	102.3	101.7	101.6
AA6061+ 10 vol.% TiB_2	150.6	151.6	154.7	152.3

Table 2. *Tensile strength of MMC*

Sample	Tensile strength, MPa
AA6061+ 5 vol.% TiB_2	142.4
AA6061+ 10 vol.% TiB_2	195.1

Design of experiments

The Box-Behnken design (BBD) is a second-order response surface methodology (RSM) model that is the focus of most RSM research [29]. The BBD only requires three levels for each element to fit a second-order regression model (quadratic). The BBD chose a middle ground between the components' initial low and high levels [47-49]. Face points, rather than corner points, are used in the BBD, resulting in fewer experimental runs. The experiments were designed using the BBD approach with Design expert software 7.0.0 version and three process parameters with 17 runs to examine the impact of EDM parameters on MRR.

- Peak current (A), three levels 1, 2, 3 at 3, 4, and 5 A
- Pulse on time (B), three levels 1, 2, 3 at 10, 15, and 20 µs
- Voltage gap (C), three levels 1, 2, 3 at 15, 30, and 45 V

A Die sinking EDM of Electronica, Pune, India, with model Electrica RT 20, was used to conduct the testing. It has a work tank that measures 650×400×280 mm and a working table that moves 200 mm in the *x*-direction, 280 mm in the *y*-direction, and 300 mm in the *z*-direction. The MMC of AA 6061 + 5 vol.% TiB_2 and AA6061 + 10 vol.% reinforcement has a 50 mm outer diameter, and two cylindrical rods with diameters of 23 mm and cylindrical rod slices of 3 mm were produced from this casting using wire cut EDM with brass wire, 0.25 mm diameter, wire tension of 7 to 8 N, and distilled water as a dielectric. As a result, the EDM machining raw material is 23×3 mm in size. The copper electrode was 4 mm in diameter. The dielectric fluid was Gandhar oil refinery Limited's Divyol SEO 25 oil, with flash and fire points of 112 and 124 °C, respectively. At 20 and 40 °C, the fluid has a viscosity of 3.48 and 2.35 $mm^2\ s^{-1}$, respectively, and a boiling point of 240 °C.

Measurement of tool wear rate

TWR was calculated for each experimental trial using the weight loss method during EDM machining, as shown in Equation (1) [30]. A computerized mass balance with a 0.001 g precision is used to estimate the beginning and end weights of the specimens. Each test sample's measurements were taken three times to ensure accuracy.

$$\mathrm{TWR} = \frac{w_{\mathrm{initial}} - w_{\mathrm{final}}}{\rho\tau} \quad (1)$$

were w is weight, ρ is density, τ is time

Results and discussion

Modelling and ANOVA of tool wear rate

The response surface methodology (RSM) was utilized to develop a model [50,51] for TWR while EDM machined AA6061 + TiB_2 MMC material. TWR could be estimated using the mathematical

model of peak current *A*, pulse on time *B*, and voltage gap *C*. To construct quadratic TWR models, the test plans were created. TWR was parametrically characterized, and a link to machining parameters was attempted. The developed TWR model for AA 6061 + 5 vol.% TiB_2 is shown by Equation (2) and for TWR AA6061 + 10 vol.% TiB_2 in Equation (3). The model's relevance, the importance of distinct aspects, and the lack of fit were determined using statistical testing.

$$\text{TWR (AA 6061+ 5 vol.\% TiB}_2) = 0.25 + 0.025A + 2.875\times10^{-3}B - 5.000\times10^{-4}C - \\ - 0.016A + 0.013AC - 10^{-3}B + 0.018A^2 + 0.019B^2 - 0.013C^2 \quad (2)$$

$$\text{TWR (AA6061 + 10 vol.\% TiB}_2) = 0.23 + 0.069A + 8.500\times10^{-3}B + 1.750\times10^{-3}C + \\ + 2.750\times10^{-3}AB - 2.500\times10^{-4}AC - 5.750\times10^{-3}BC + 0.024A^2 - 2.975\times10^{-3}B^2 + 2.500\times10^{-5}C^2 \quad (3)$$

ANOVA is a family of standardized models and accompanying estimates processes for analyzing differences between means [52,53]. It's used in various settings to see if there's a significant difference between means of distinct groups [54-56]. For example, Table 3 shows ANOVA for TWR: RSM for TWR of 5 vol.% TiB_2 (Partial sum of squares-type III). Table 4 shows ANOVA for TWR: RSM model for TWR of 10 vol.% TiB_2 (Partial sum of squares-type III).

Table 3. *ANOVA for TWR: RSM for TWR of 5 vol.% TiB_2 (Partial sum of squares - type III)*

Source	Sum of squares	df	Mean square	F value	*p*-value - prob>*F*	
Model	0.010	9	1.134×10^{-3}	35.56	< 0.0001	Significant
A	4.950×10^{-3}	1	4.950×10^{-3}	155.21	< 0.0001	Significant
B	6.613×10^{-5}	1	6.613×10^{-5}	2.07	0.1931	
C	2.000×10^{-6}	1	2.000×10^{-6}	0.063	0.8095	
AB	1.056×10^{-3}	1	1.056×10^{-3}	33.12	0.0007	Significant
AC	7.290×10^{-1}	1	7.290	22.86	0.0020	Significant
BC	4.000×10^{-6}	1	4.000×10^{-6}	0.13	0.7337	
Residual	2.233×10^{-4}	7	3.189×10^{-5}	--	--	
Lack of fit	4.525×10^{-5}	3	1.508×10^{-5}	0.34	0.7996	Non-Significant
Pure error	1.780×10^{-4}	4	4.450×10^{-5}	--	--	
Cor total	0.010	16	--	--	--	
Std. dev.	5.647×10^{-3}	--	--	R^2	0.9786	
Mean	0.26	--	--	Adj R^2	0.9511	
CV, %	2.19	--	--	Pred R^2	0.9039	
PRESS	1.002×10^{-3}	--	--			

The model *F*-values of 35.56 and 72.21, respectively, indicate that the model is significant for 5 and 10 vol.% TiB_2. Due to noise, there is only a 0.01 % chance that a "model *F*-value" this large will occur. The EDM parameters' significance is revealed by *p* values less than 0.05. TWR of 5 vol.% TiB_2 *A*, *AB*, and *AC* are significant, but TWRs of 10 vol.% TiB_2 *A* and *B* are significant. The lack of non-significant results in the developed modes indicates they are good. *F*-values of 0.34 and 0.52 for TWR of 5 vol.% TiB_2 and 10 vol.% TiB_2 show no substantial lack of fit. The lack of fit at 5 vol.% TiB_2 may be attributed to noise in 79.96 % of cases and at 10 vol.% TiB_2 in 68.95 % of cases. Excellent concordance is seen between the observed R-square values of 0.9511 for 5 vol.% TiB_2 and 0.9756 for 10 vol.% TiB_2 and the expected values of 0.9039 and 0.9400, respectively.

Table 4. *ANOVA for TWR: RSM model for TWR of 10 vol.% TiB_2 (Partial sum of squares - type III)*

Source	Sum of squares	df	Mean square	*F* value	*p*-value - prob>*F*	
Model	0.041	9	4.578×10^{-3}	72.21	< 0.0001	Significant
A	0.038	1	0.038	600.76	< 0.0001	Significant
B	5.780×10^{-4}	1	5.780×10^{-4}	9.12	0.0194	Significant
C	2.450×10^{-5}	1	2.450×10^{-5}	0.39	0.5539	
AB	3.025×10^{-5}	1	3.025×10^{-5}	0.48	0.5120	
AC	2.500×10^{-7}	1	2.500×10^{-7}	3.943E-003	0.9517	
BC	1.323×10^{-4}	1	1.323×10^{-4}	2.09	0.1919	
Residual	4.438×10^{-4}	7	6.340×10^{-5}	--	--	
Lack of fit	1.250×10^{-4}	3	4.167×10^{-5}	0.52	0.6895	Non- Significant
Pure error	3.188×10^{-4}	4	7.970×10^{-5}	--	--	
Cor total	0.042	16	--	--	--	
Std. dev.	7.962×10^{-3}	-	--	R^2	0.9893	
Mean	0.24	--	--	Adj R^2	0.9756	
CV, %	3.28	--	--	Pred R^2	0.9400	
PRESS	2.498×10^{-3}	--	--			

Assessment of actual and predicted TWR

The predicted versus actual responses were displayed to verify the appropriateness of the created model. The RSM model's effectiveness for the replies was assessed by inserting the data into the constructed model [57,58]. The experimental results are compared to the predicted data from the analysis, as shown in Figure 3.

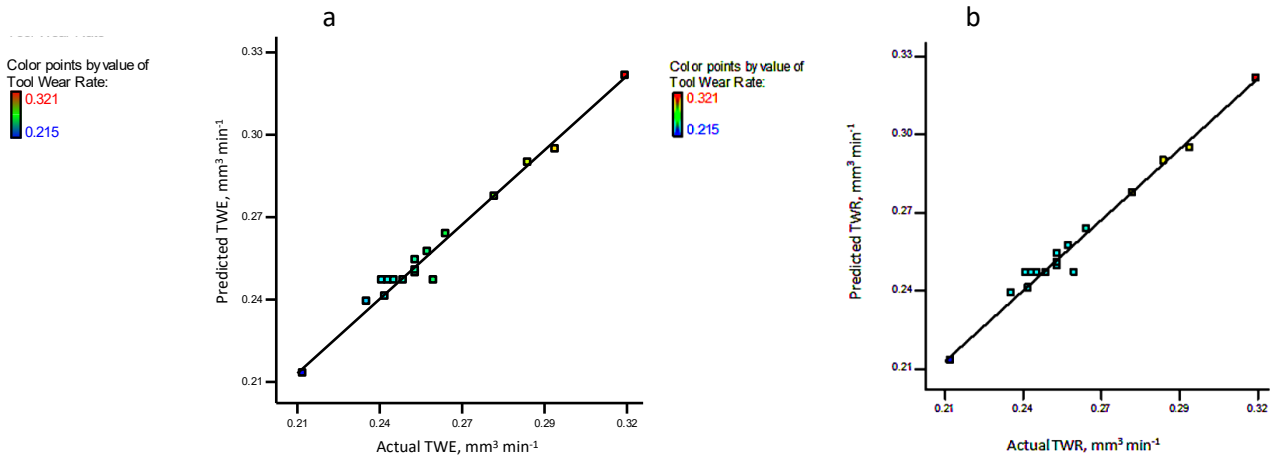

Figure 3. *Plots for TWR (a) AA6061 + 5 vol.% TiB_2(MMC) and (b) AA 6061 + 10 vol.% TiB_2 (MMC)*

The proposed quadratic models for responses performed admirably, with a little lack of fit, and had no difficulty predicting response values, as indicated by the smallest range of projected data points in both situations. The anticipated value points were uniformly distributed, near the parity line, and fit in a straight line. The model robustness gains confidence as a result of this.

Normal probability plots

A normal probability map is a visual tool detecting significant deviations from normality. Examples include outliers, skewness, kurtosis, the need for transformations, and mixtures. They are raw data, model fit residuals, and predicted variables [59-61]. If the data are roughly normally distributed, the sorted data are plotted versus values chosen to make the final image look near a straight line. Variations from a straight line indicate discrepancies [51,62]. For example, the normal

probability plot of residuals for TWR for AA6061 + 5 vol.% TiB_2 MMC is shown in Figure 4(a) and for TWR for AA6061 + 10 vol.% TiB_2 MMC in Figure 4(b). Most plotted points form a reasonably linear pattern, with minimal deviations from the straight line indicating consistent data, indicating the model competence.

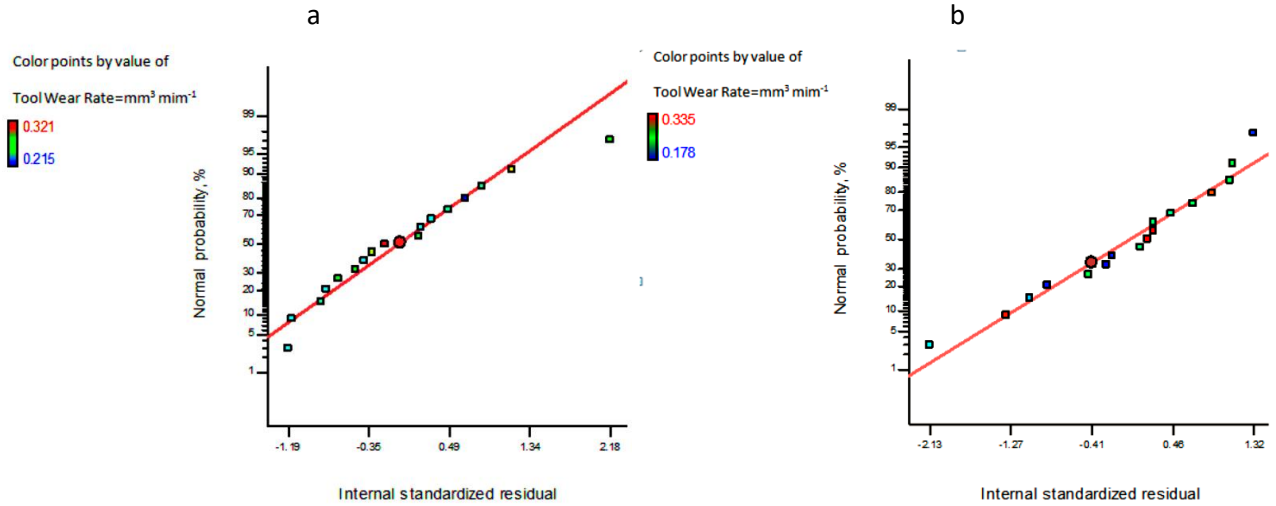

Figure 4. *Normal probability plots for TWR (a) AA6061 + 5 vol.% TiB_2 (MMC), (b) AA 6061 + 10 vol.% TiB_2 (MMC)*

Optimization of EDM for developed MMC by desirability analysis

Desirability analysis solutions for TWR for 5 and 10 vol.% TiB_2 are shown in Table 5, with the top five results to choose the best value.

Table 5. *Desirability Solutions for TWR*

Number	Current, A	Time, µs	Voltage, V	TWR, mm^3 min^{-1}	Desirability	
AA6061 + 5 vol.%TiB_2						
1.	3.32	14.01	44.73	0.2146	1.000	selected
2.	3.30	14.09	44.68	0.2145	1.000	
3.	3.02	13.32	43.35	0.2134	1.000	
4.	3.11	12.99	44.35	0.2117	1.000	
5.	3.04	14.27	44.11	0.2133	1.000	
AA6061 + 10 vol.%TiB_2						
1.	3.13	10.16	15.59	0.1749	1.000	selected
2.	3.00	10.92	18.67	0.1760	1.000	
3.	3.08	10.06	21.98	0.1768	1.000	
4.	3.05	11.26	17.90	0.1777	1.000	
5.	3.02	10.49	21.91	0.1767	1.000	

The optimal value for MMC of AA 6061 + 5 vol.% TiB_2 has a current of 3.32 A, a duration of 14.01 µs, and a voltage gap of 44.73 V, resulting in a TWR of 0.2146 mm^3min^{-1}. An optimal value for the MMC of AA6061 + 10 vol.% TiB_2, with a current of 3.13 A and a time of 10.16 µs with a voltage gap of 15.59 V, yields a TWR of 0.1749 mm^3min^{-1}.

Perturbation plot

The perturbation plot can be used to compare all the components' effects at a single point in the solution space. Only one parameter is changed across the response spectrum, while the others remain constant. For example, Figure 5 shows the perturbation plot for TWR of AA6061 + 5 vol.%

TiB_2 and AA6061 + 10 vol.% TiB_2, where *A* represents peak current, *B* represents pulse on time, and *C* indicates voltage gap. TWR rises as current rises, and pulse on-time slightly impacts TWR, whereas voltage has a much smaller impact.

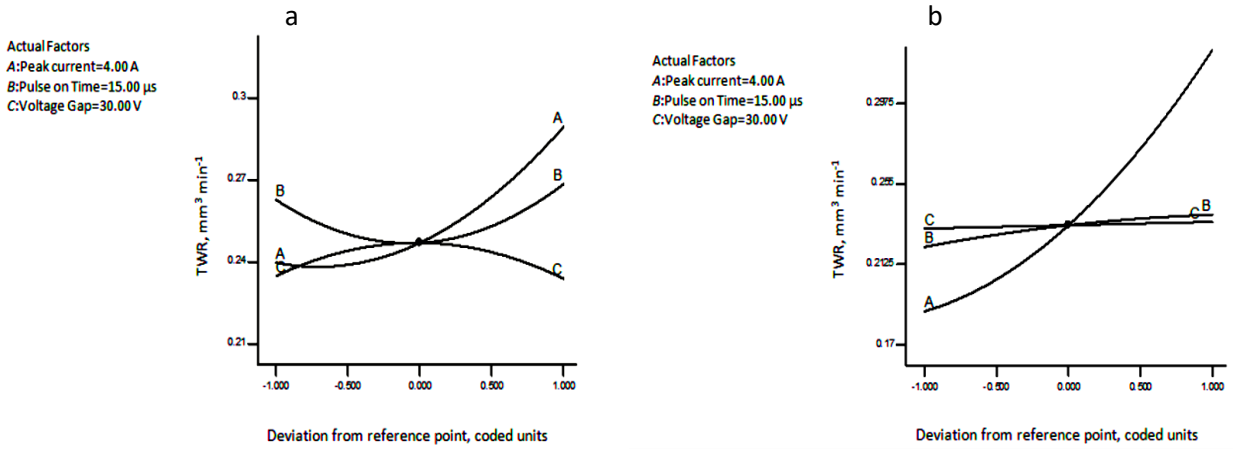

Figure 5. *Perturbation plots for TWR (a) AA6061 + 5 vol.% TiB_2 (MMC); (b) AA 6061 + 10 vol.% TiB_2 (MMC)*

Contour plots

A contour plot is a graphical technique for displaying a 3-dimensional surface in a 2-dimensional format by showing contours. A contour plot is a 2-D version of a 3-D surface plot [63-65]. For example, it is evident from Figure 6 for 5 and 10 vol.% TiB_2 that as the current and time increase, there is an increase in the tool wear. Furthermore, it is evident from Figures 6(a) and 6(b) that with the increase in the current tool wear rate increases, the blue area indicates less TWR, and the red indicates more TWR.

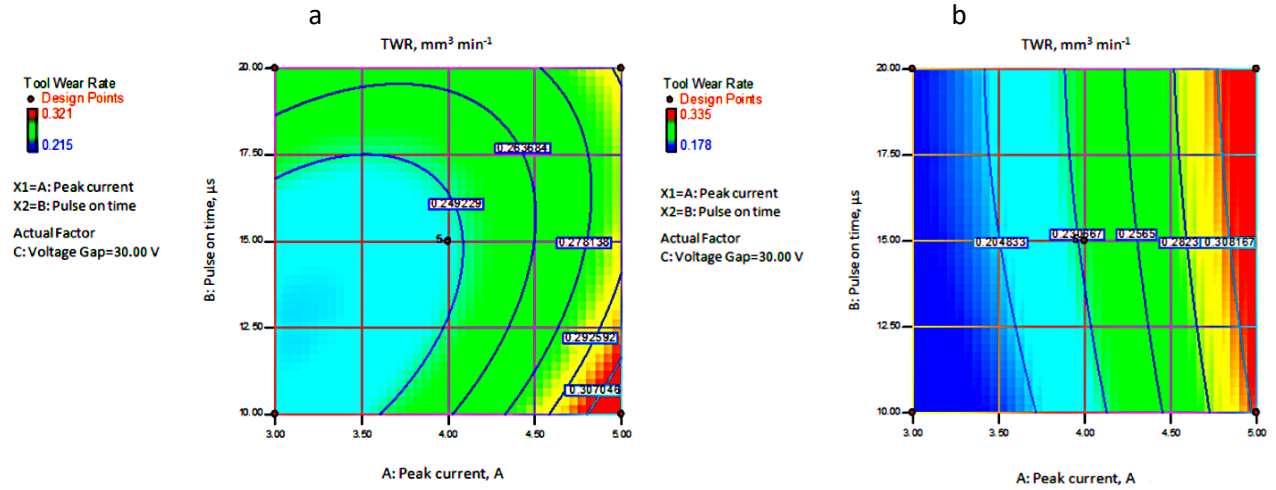

Figure 6. *Contourplots for TWR (a) AA6061 TiB_2 (5 vol.%) MMC, (b) AA 6061 TiB_2 (10 vol.%) MMC*

Surface roughness at optimal variables and comparative analysis

The tool wear and surface roughness for 5 vol.% TiB_2 is 0.2146 mm^3min^{-1} and 2.47 µm, respectively. Tool wear and surface roughness for 10 vol.% TiB_2 is 0.1749 mm^3min^{-1} and 3.03 µm. Therefore, it indicates that as the reinforcement grows, the tool wear and surface roughness decreases, indicating that as the reinforcement increases, the MRR decreases, directly affecting the TWR and R_a; similar results were also reported [55,56]. The comparative results for TWR, R_a, hardness and tensile strength are shown in Figure 7 and optimal EDM variables.

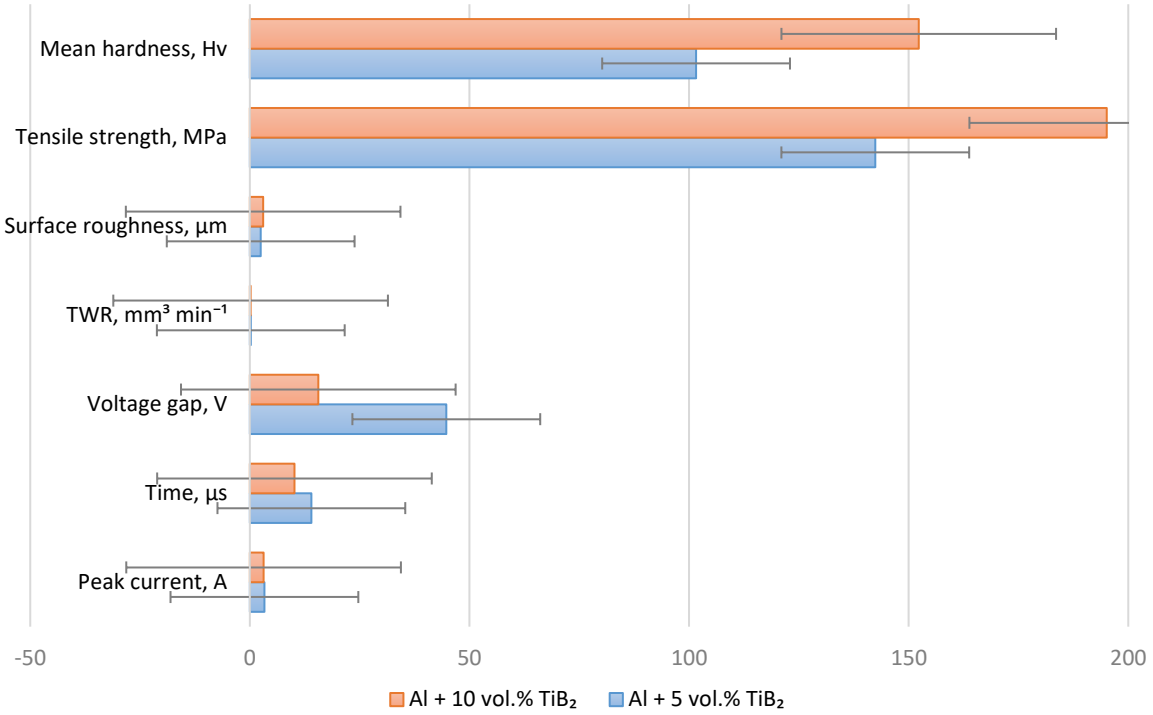

Figure 7. *Comparative results for AA6061 + TiB_2 (5 vol.%) MMC, and AA 6061 + TiB_2 (10 vol.%) MMC*

Conclusions

Squeeze casting made the Al alloy 6061 MMCs with 5 and 10 vol.% TiB_2 reinforcements. Squeeze cast specimens have less porosity than squeezing because they are created with a squeeze motion. Chemical composition revealed by microstructure and EDS analysis included Ti, Boron, and other elements. Because of its exceptional characteristics, Al MMC has a well-known use. The experiments were designed using the BBD approach to explore the impact of EDM parameters, including peak current, pulse on time, and voltage gap on TWR. Various analyses of TWR's optimization and modelling lead to meaningful results.

- The results of Squeeze casting reveal that when the TiB_2 increased from 5 to 10 vol.%, the hardness increased from 101.6 to 152.3 Hv, while tensile strength increased from 142.4 to 195.1 MPa, respectively.
- The EDM parameters for MMC of AA 6061 + TiB_2 with 5 and 10 vol.% reinforcement casting reveal that as the current increases, so does the surface roughness. In addition, TWR was observed to rise when pulse on time increased.
- The RSM *F*-values of 35.56 for TWR of 5 vol.% TiB_2 and 72.21 for TWR of 10 vol.% TiB_2 indicate that the model is significant, and the predicted R^2 of 0.9039for TWR of 5 vol.% TiB_2, and 0.9400 for TWR of 10 vol.% TiB_2 are in reasonable agreement with the corrected R^2 of 0.9511 and 0.9756, respectively.
- Desirability analysis reveals that the optimal value for MMC of AA 6061 + 5 vol.% TiB_2 has a peak current of 3.32 A, pulse on time of 14.01 µs, and a voltage gap of 44.73 V, giving a TWR of 0.2146 mm^3min^{-1}. An optimal value for the MMC of AA6061 + 10 vol.% TiB_2 with a peak current of 3.13 A and a pulse on time of 10.16 µs with a voltage gap of 15.59 V produces a TWR of 0.1749 mm^3min^{-1}.

Acknowledgements: *The authors express deep gratitude to I. K. Gujral Punjab Technical University, Kapurthala-Jalandhar (Punjab), India, for allowing them to carry out this research work.*

References

[1] S. Lakshmi, L. Lu, M. Gupta, *Journal of Materials Processing Technology* **73(1)** (1998) 160-166. https://doi.org/10.1016/S0924-0136(97)00225-2

[2] S. Natarajan, R. Narayanasamy, S. P. Kumaresh Babu, G. Dinesh, B. Anil Kumar, K. Sivaprasad, *Materials & Design* **30(7)** (2009) 2521-2531. https://doi.org/10.1016/j.matdes.2008.09.037

[3] N. Ehsania, F. Abdib, H. Abdizadehc, H. R. Baharvandid, *International Conference on Smart Materials and Nanotechnology in Engineering,* Proceedings **6423** (2008) 642369. https://doi.org/10.1117/12.791738

[4] J. Hashim, *Jurnal Teknologi* **35(A)**(2001) 9-20. https://doi.org/10.11113/jt.v35.588

[5] B. Bobić, S. Mitrovic, M. Babic, I. Bobić, *Tribology in Industry* **32** (2010) 3-11. http://www.tribology.rs/journals/2010/2010-1/1.pdf

[6] S. C. Tjong, K. F. Tam, *Materials Chemistry and Physics* **97(1)** (2006) 91-97. https://doi.org/10.1016/j.matchemphys.2005.07.075

[7] S. Suresh, N. Shenbaga Vinayaga Moorthi, S. C. Vettivel, N. Selvakumar, *Materials & Design* **59** (2014) 383-396. https://doi.org/10.1016/j.matdes.2014.02.053

[8] A. Baradeswaran,A. Elaya Perumal, *Composites Part B: Engineering* **54** (2013) 146-152. https://doi.org/10.1016/j.compositesb.2013.05.012

[9] C. S. Ramesh, S. Pramod, R. Keshavamurthy, *Materials Science and Engineering: A* **528(12)** (2011) 4125-4132. https://doi.org/10.1016/j.msea.2011.02.024

[10] A. Torres, C. J. Luis, I. Puertas, *Procedia Manufacturing* **13** (2017) 579-584. https://doi.org/10.1016/j.promfg.2017.09.104

[11] N. Eliaz,N. Metoki, *Materials* **10(4)** (2017) 334. https://doi.org/10.3390/ma10040334

[12] V. Guarino, M. Iafisco, S. Spriano, *Nanostructured Biomaterials for Regenerative Medicine*, Woodhead Publishing, Napoli, Italy 2020, p. 1-27.

[13] T. J. Kinnari, J. Esteban, E. Gomez-Barrena, N. Zamora, R. Fernandez-Roblas, A. Nieto, J. C. Doadrio, A. López-Noriega, E. Ruiz-Hernández, D. Arcos, M. Vallet-Regí, *Journal of Biomedical Material Research Part A* **89A(1)** (2009) 215-223. https://doi.org/10.1002/jbm.a.31943

[14] J. Park, *Bioceramics: Properties, Characterizations, and Applications*, Springer Science & Business Media, lowa City, USA 2009, p.363. https://doi.org/10.1007/978-0-387-09545-5

[15] M. Semlitsch, M. Lehmann, H. Weber, E. Doerre, H. G. Willert, *Journal of Biomedical Materials Research* **11(4)** (1977) 537-552. https://doi.org/10.1002/jbm.820110409

[16] C. Combes, C. Rey, Bioceramics in *Ceramic Materials*, Philippe Boch, Jean-Claude Niepce, ISTE Ltd London, UK 2007, p. 493-521.

[17] R. Kumar, R. Dubey, S. Singh, S. Singh, C. Prakash, Y. Nirsanametla, G. Królczyk, R. Chudy *Materials* **14(8)** (2021) 2084. https://www.mdpi.com/1996-1944/14/8/2084

[18] C. Prakash, P. Senthil, N. Manikandan, D. Palanisamy, *Materials and Manufacturing Processes* **37(7)** (2022) 748-763. https://doi.org/10.1080/10426914.2021.1962531

[19] H. Nair, A. Pramanik, A. K. Basak, C. Prakash, S. Debnath, S. Shankar, A. R. Dixit, *Proceedings of the Institution of Mechanical Engineers, Part E: Journal of Process Mechanical Engineering* (2022). https://doi.org/10.1177/09544089221096025

[20] P. Haja Syeddu Masooth, G. Bharathiraja, V. Jayakumar, K. Palani, *Materials Research Express* **9(4)** (2022) 046521. https://doi.org/10.1088/2053-1591/ac672d

[21] P. Haja Syeddu Masooth, V. Jayakumar, G. Bharathiraja, *Materials Today: Proceedings* **22** (2020) 726-736. https://doi.org//10.1016/j.matpr.2019.10.036

[22] M. Das, K. Kumar, T. Barman, P. Sahoo, *Procedia Materials Science* **6** (2014) 741-751. https://doi.org/10.1016/j.mspro.2014.07.090

[23] M. Dastagiri A. H. Kumar, *Procedia Engineering* **97** (2014) 1551-1564. https://doi.org/10.1016/j.proeng.2014.12.439

[24] M. Durairaj, D. Sudharsun, N. Swamynathan, *Procedia Engineering* **64** (2013) 868-877. https://doi.org/10.1016/j.proeng.2013.09.163

[25] M. Azadi Moghaddan, F. Kolahan, *International Journal of Engineering* **27(3)** (2014) 417-424.

[26] A. K. Bodukuri, S. Chandramouli, K. Eswaraiah, J. Laxman, *Materials Today: Proceedings* **5(11,3)** (2018) 24731-24740. https://doi.org/10.1016/j.matpr.2018.10.271

[27] S. Mohanty, B. C. Routara, R. K. Bhuayan, *Materials Today: Proceedings* **4(8)** (2017) 8778-8787. https://doi.org/10.1016/j.matpr.2017.07.227
[28] S. Mahanta, M. Chandrasekaran, S. Samanta, *Materials Today: Proceedings* **5(2)** (2018) 7788-7796. https://doi.org/10.1016/j.matpr.2017.11.457
[29] K. R. Aharwal, Sitaram, C. M. Krishna, *Materials Today: Proceedings* **5(2,1)** (2018) 5391-5397. https://doi.org/10.1016/j.matpr.2017.12.125
[30] N. Radhika, S. Addamane, G. Chandran, *Journal of Engineering Science and Technology* **9** (2014) 502-512.
[31] M. Prabu, G. Ramadoss, P. Narendersingh, T. V. Christy, V. V. Eswaran, *Science and Engineering of Composite Materials* **21(3)** (2014) 445-452. https://doi.org/doi:10.1515/secm-2013-0023
[32] P. Senthil, S. Vinodh, A. Singh, *International Journal of Machining and Machinability of Materials* **16** (2014) 80-94. https://doi.org/10.1504/IJMMM.2014.063922
[33] R. Kumar H. K. Channi, *Journal of Cleaner Production* **349** (2022) 131347. https://doi.org/10.1016/j.jclepro.2022.131347
[34] A. S. Walia, V. Srivastava, M. Garg, N. Somani, N. K. Gupta, C. Prakash, C. Bhargava, K. Kotecha, *Materials* **14(20)** (2021) 5943. https://doi.org/10.3390/ma14205943
[35] A. Sharma, V. Kumar, A. Babbar, V. Dhawan, K. Kotecha, C. Prakash, *Materials* **14(19)** (2021) 5820 . https://doi.org/10.3390/ma14195820
[36] A. Pramanik, A. K. Basak, C. Prakash, S. Shankar, S. Sharma, S. Narendranath, *Journal of Materials Engineering and Performance* **30(12)** (2021) 8926-8935. https://doi.org/10.1007/s11665-021-06116-1
[37] M. Dutt Sharma, R. Sehgal, M. Pant, *Journal of Tribology* **138(3)** (2016) 031603. https://doi.org/10.1115/1.4032518
[38] C. Prakash, H. K. Kansal, B. S. Pabla, S. Puri, *Journal of Materials Engineering and Performance* **24(9)** (2015) 3622-3633. https://doi.org/10.1007/s11665-015-1619-6
[39] C. Prakash, H. K. Kansal, B. S. Pabla, S. Puri, *Journal of Computing and Information Science in Engineering* **16(4)** (2016) 041006. https://doi.org/10.1115/1.4033901
[40] C. Prakash, H. K. Kansal, B. S. Pabla, S. Puri, *Nanoscience and Nanotechnology Letters* **8(10)** (2016) 815-826. https://doi.org/10.1166/nnl.2016.2255
[41] C. Prakash, H. K. Kansal, B. S. Pabla, S. Puri, *Journal of Mechanical Science and Technology* **30(9)** (2016) 4195-4204. https://doi.org/10.1007/s12206-016-0831-0
[42] H. Kaur Channi, M. Singh, Y. Singh Brar, A. Dhingra, S. Gupta, H. Singh, R. Kumar, S. Kaur, *Materials Today: Proceedings* **50(5)** (2022) 700-708. https://doi.org/10.1016/j.matpr.2021.04.481
[43] C. Prakash, H. K. Kansal, B. S. Pabla, S. Puri, A. Aggarwal, *Proceedings of the Institution of Mechanical Engineers, Part B: Journal of Engineering Manufacture* **230(2)** (2016) 331-353. https://doi.org/10.1177/0954405415579113
[44] A. A. Aliyu, A. M. Abdul-Rani, T. L. Ginta, C. Prakash, E. Axinte, M. A. Razak, S. Ali, *Advances in Materials Science and Engineering* **2017** (2017) 8723239. https://doi.org/10.1155/2017/8723239
[45] C. Prakash, H. K. Kansal, B. S. Pabla, S. Puri, *Materials and Manufacturing Processes* **32(3)** (2017) 274-285. https://doi.org/10.1080/10426914.2016.1198018
[46] C. Prakash M. S. Uddin, *Surface and Coatings Technology* **326** (2017) 134-145. https://doi.org/10.1016/j.surfcoat.2017.07.040
[47] C. Prakash, S. Singh, B. S. Pabla, M. S. Uddin, *Surface and Coatings Technology* **346** (2018) 9-18. https://doi.org/10.1016/j.surfcoat.2018.04.035
[48] C. Prakash, S. Singh, M. Singh, K. Verma, B. Chaudhary, S. Singh, *Vacuum* **158** (2018) 180-190. https://doi.org/10.1016/j.vacuum.2018.09.050
[49] A. Pramanik, M. N. Islam, A. K. Basak, Y. Dong, G. Littlefair, C. Prakash, *Materials and Manufacturing Processes* **34(10)** (2019) 1083-1090. https://doi.org/10.1080/10426914.2019.1628259
[50] K. K. Goyal, N. Sharma, R. D. Gupta, G. Singh, D. Rani, H. K. Banga, R. Kumar, D. Y. Pimenov, K. Giasin, *Materials* **15(2)** (2022) 635. https://doi.org/10.3390/ma15020635
[51] A. S. Sidhu, S. Singh, R. Kumar, D. Y. Pimenov, K. Giasin, *Energies* **14(16)** (2021) 4761. https://doi.org/10.3390/en14164761

[52] S. Singh, R. Kumar, R. Kumar, J. S. Chohan, N. Ranjan, R. Kumar, *Proceedings of the Institution of Mechanical Engineers, Part L: Journal of Materials: Design and Applications* **236(3)** (2022) 674-691. https://doi.org/10.1177/14644207211054143
[53] R. Kumar, S. Singh, V. Aggarwal, S. Singh, D. Y. Pimenov, K. Giasin, K. Nadolny, *Materials* **15(4)** (2022) 1287. https://doi.org/10.3390/ma15041287
[54] P. Antil, S. Kumar Antil, C. Prakash, G. Królczyk, C. Pruncu, *Measurement and Control (United Kingdom)* **53(9-10)** (2020) 1902-1910. https://doi.org/10.1177/0020294020947126
[55] A. Kumar, N. Grover, A. Manna, J. S. Chohan, R. Kumar, S. Singh, C. Prakash, C. I. Pruncu, *Advanced Composites Letters* **29** (2020). https://doi.org/10.1177/2633366x20963137
[56] A. Basak, A. Pramanik, C. Prakash, K. Kotecha, *Materials Letters* **305** (2021) 130769. https://doi.org/10.1016/j.matlet.2021.130769
[57] G. Singh, S. Singh, C. Prakash, R. Kumar, R. Kumar, S. Ramakrishna, *Polymer Composites* **41(9)** (2020) 3871-3891. https://doi.org/10.1002/pc.25683
[58] K. Sandhu, G. Singh, S. Singh, R. Kumar, C. Prakash, S. Ramakrishna, G. Królczyk, C. I. Pruncu, *Materials,* **13(12)** (2020) 2729. https://doi.org/10.3390/ma13122729
[59] R. Kumar, S. Singh, P. S. Bilga, Jatin, J. Singh, S. Singh, M. L. Scutaru, C. I. Pruncu, *Journal of Materials Research and Technology* **10** (2021) 1471-1492. https://doi.org/10.1016/j.jmrt.2020.12.114
[60] R. Kumar, P. S. Bilga, S. Singh, *Procedia CIRP* **98** (2021) 654-659. https://doi.org/10.1016/j.procir.2021.01.170
[61] R. S. Chandel, R. Kumar, J. Kapoor, *Materials Today: Proceedings* **50(5)** (2022) 716-727. https://doi.org/10.1016/j.matpr.2021.04.624
[62] R. Kumar, P. S. Bilga, S. Singh, *International Journal of Metallurgy Alloys* **6(1)** (2020) 37-45. https://doi.org/10.37628/ijma.v6i1.632
[63] S. Singh, R. Kumar, R. Kumar, J. S. Chohan, N. Ranjan, R. Kumar, *Proceedings of the Institution of Mechanical Engineers, Part L: Journal of Materials: Design and Applications* **236(3)** (2021) 674-691. https://doi.org/10.1177/14644207211054143
[64] R. Kumar, R. Singh, M. S. J. Hashmi, *Advances in Materials and Processing Technologies* (2022) 895-908. https://doi.org/10.1080/2374068X.2020.1835013
[65] G. Singh, S. Singh, C. Prakash, R. Kumar, R. Kumar, S. J. P. C. Ramakrishna, *Polymer Composites* **41(9)** (2020) 3871-3891. https://doi.org/https://doi.org/10.1002/pc.25683